Geomorphology 273 (2016) 269–279

Contents lists available at ScienceDirect

Geomorphology

journal homepage: www.elsevier.com/locate/geomorph

# Identification of debris-flow hazards in warm deserts through analyzing past occurrences: Case study in South Mountain, Sonoran Desert, USA

Ronald I. Dorn

*School of Geographical Sciences & Urban Planning, Arizona State University, Tempe, AZ 85287-5302, USA*

ARTICLE INFO

*Article history:*
Received 14 March 2016
Received in revised form 7 August 2016
Accepted 8 August 2016
Available online 16 August 2016

*Keywords:*
Alluvial fan
Desert geomorphology
Eolian
Landslide
Mass wasting

ABSTRACT

After recognition that debris flows co-occur with human activities, the next step in a hazards analysis involves estimating debris-flow probability. Prior research published in this journal in 2010 used varnish microlamination (VML) dating to determine a minimum occurrence of 5 flows per century over the last 8100 years in a small mountain range of South Mountain adjacent to neighborhoods of Phoenix, Arizona. This analysis led to the conclusion that debris flows originating in small mountain ranges in arid regions like the Sonoran Desert could pose a hazard. Two major precipitation events in the summer of 2014 generated 35 debris flows in the same study area of South Mountain—providing support for the importance of probability analysis as a key step in a hazards analysis in warm desert settings. Two distinct mechanisms generated the 2014 debris flows: intense precipitation on steep slopes in the first storm; and a firehose effect whereby runoff from the second storm was funneled rapidly by cleaned-out debris-flow chutes to remobilize Pleistocene debris-flow deposits. When compared to a global database on debris flows, the 2014 storms were among the most intense to generate desert debris flows — indicating that storms of lesser intensity are capable of generating debris flows in warm desert settings. The $^{87}Sr/^{86}Sr$ analyses of fines and clasts in South Mountain debris flows of different ages reveal that desert dust supplies the fines. Thus, wetter climatic periods of intense rock decay are not needed to resupply desert slopes with fines; instead, a combination of dust deposition supplying fines and dirt cracking generating coarse clasts can re-arm chutes in a warm desert setting with abundant dust.



## 1. Introduction

A debris-flow hazard analysis starts with recognition that debris flows could occur near the built environment (Jakob and Hungr, 2005). This first step is then followed by estimation of debris-flow probability (Jakob, 2005; Hürlimann et al., 2006; Miller and Burnett, 2008) using different strategies such as modeling (Miller and Burnett, 2008; De Paola et al., 2015; Gartner et al., 2015), rainfall probability analysis (Lee et al., 2016; Yu et al., 2016), or empirical approaches employing dating techniques to reconstruct past occurrences such as dendrogeomorphology (Butler et al., 1987; Tichavský and Šilhán, 2015), radiocarbon (Sewell et al., 2015), historical photographs (Dietrich et al., 2016), and cosmogenic nuclides (Fuchs et al., 2015).

Although debris flows commonly occur in arid and semiarid regions (Hooke, 1967; Yair and Klein, 1973; Blair and McPherson, 2009), hazards research on debris flows tends to focus in wetter regions (Jakob and Hungr, 2005). Still, as urban centers in drylands expand against mountains, debris flows are increasingly recognized as potential hazards in deserts (Webb et al., 2013) such as Argentina (Moreiras, 2006), Chile (Sepulveda et al., 2006), China (Zhou et al., 2016), India (Stolle et al., 2015), Iran (Beaumont, 1972), Pakistan (Shaw, 2015), and rural settings such as farmed terraces in a wide variety of arid and semiarid settings globally (Arnáez et al., 2015).

In the Sonoran Desert, however, the guide to geological hazards for home buyers in Arizona, USA, reflects the general perception that debris flows are remnants wetter glacial conditions (Melton, 1965) and not relevant to a Sonoran desert setting with rare and sporadic rainfall (Harris and Pearthree, 2002). This perception did change, though, after a major 2006 precipitation event generated debris flows reaching the doorstep of Tucson (Youberg et al., 2008), AZ — leading to the view debris flows might be an underappreciated hazard in southern Arizona (Pearthree et al., 2007).

In this context of uncertainty as to the potential for debris flows as a geomorphological hazard in urban settings in the Sonoran Desert, chronometric data from varnish microlaminations (VML) assessed the minimum occurrences of debris flows on the north side of the Ma Ha Tuak range of South Mountain, Sonoran Desert, bordering Phoenix AZ; a minimum of 5 debris flows per century occurred over the last 8100 years (Dorn, 2010). Further analyses revealed that a potential hazard exists for homes underneath debris-flow chutes on debris-flow deposits (Dorn, 2012; Moore et al., 2012).

A few years after publication (Dorn, 2010, 2012; Moore et al., 2012), two major precipitation events took place in 2014 only 27 days apart in

*E-mail address:* ronald.dorn@asu.edu.

http://dx.doi.org/10.1016/j.geomorph.2016.08.013
0169-555X/

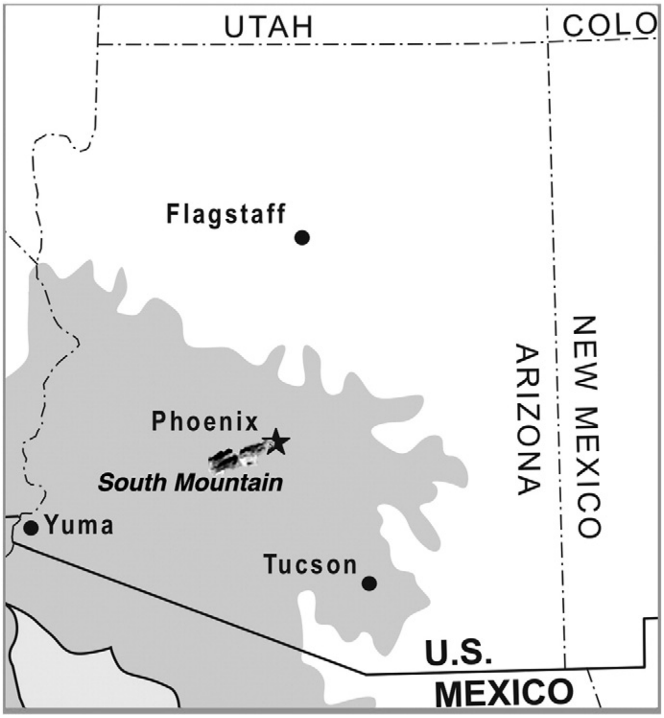


**Fig. 1.** South Mountain placed in the context of the shaded area of the Sonoran Desert, Arizona, USA.

the same Phoenix, AZ, study area of South Mountain. An intense summer thunderstorm event occurred on 12 August (Flood Control District of Maricopa County, 2014a), followed by a long-duration soaking by hurricane moisture on 8 September 2014 (Flood Control District of Maricopa County, 2014b). These storms generated 35 debris flows at South Mountain. This paper explores this warm desert case study where determining the past occurrences of debris flows functioned well as a tool to predict debris-flow hazards on small arid mountain slopes next to urbanization.

This paper also presents new VML data to facilitate a comparison of the timing of prior debris flows from the same small catchments that failed in 2014. This comparison highlights the need for multiple study sites to understand debris-flow prior occurrence in small desert ranges because different basins in the same range may have different paleodebris flow ages. Thus, compiling data from multiple basins provides a more comprehensive picture of paleodebris flow events that can then be used to understand probability of occurrence.

## 2. Field area

South Mountain stretches ~29 km in length and is a city preserve located in the Sonoran Desert within the city boundaries of Phoenix, AZ (Fig. 1). South Phoenix, Laveen, and Awahtukee neighborhoods of Phoenix border this metamorphic core complex (Fig. 2). The western half consists mainly of Precambrian gneiss (Xm in Fig. 2), while the eastern portion consists of mid-Tertiary plutonic lithologies (Tg in Fig. 2). South Mountain originated from crustal extension after the Mesozoic Sevier and Laramide orogenies (Nations and Stump, 1981; Coney and Harms, 1984; Holt et al., 1986). South Mountain's uplift ended ~8–14 Ma ago (Spencer, 1984; Reynolds, 1985).

Debris flows dominate sediment transport on the steep (Fig. 3) gneissic slopes of the Ma Ha Tuak and Gila Ranges. Evidence comes in the form of a series of debris-chutes and levees (Dorn, 2010) that form the debris-flow fans upon which homes are built (Dorn, 2012; Moore et al., 2012). A likely reason why the granitic eastern half of South Mountain (Tg in Fig. 2) does not generally produce debris flows is the way that granitic rocks decay to grus (Seong et al., 2016) that is transported by overland flow (Dorn, 2015). In contrast, the gneissic western ranges at South Mountain break apart through dirt cracking (Dorn, 2011) into boulders that are transported by mass wasting processes such as rock fall, small landslides, and debris flows (Dorn, 2010).

The climate and vegetation of South Mountain is typical of the Sonoran Desert, USA. Annual precipitation averages 208 mm and is evenly divided between winter and monsoon maxima. Winter rainfall comes from Pacific low-pressure systems. Summer rainfall derives from summer thunderstorms during the July–September monsoon season where air masses come from the Gulfs of Mexico and California,

## 3. Debris-flow triggering rain events

The 12 August 2014 precipitation event that generated debris flows was an Arizona monsoon thunderstorm, where the triggering mechanism was an inverted trough from Baja California. The Arizona State Climatologist's rain gauge at South Mountain measured 26 mm in 10 min, 68 mm in 50 min and 86 mm in 100 min translating into intensities of 154, 81, and 51 mm/h (Dr. Nancy Selover, Arizona State Climatologist, personal communication, 2014). An initial analysis of radar revealed South Mountain to have been the focus of the most intense precipitation of this thunderstorm (Flood Control District of Maricopa County, 2014a).

The 8 September 2014 event that also generated debris flows was a different type of storm. Moisture from Hurricane Norbert soaked Phoenix, AZ, for over 4 h and produced more total precipitation for South Mountain than the 12 August (Flood Control District of Maricopa County, 2014b). Intensities during 8 September, however, were much

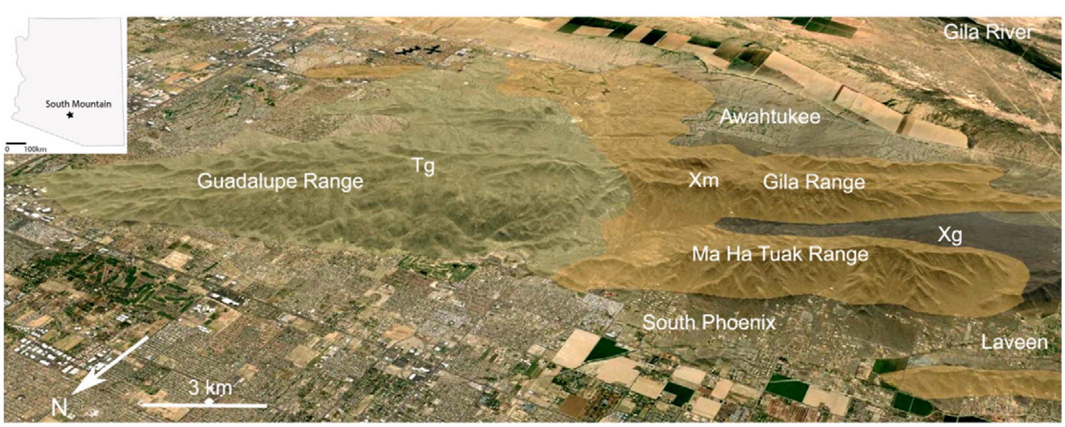


**Fig. 2.** South-east looking view of South Mountain and surrounding neighborhoods of Phoenix, AZ. The study area rests in the western portion consisting mostly of Proterozoic gneisses (Xm) with a small pocket of Proterozoic granites (Xg). Debris flows dominate hillslope transport in the gneisses, while grus transport dominates the eastern granitic hillslopes. The debris flows occurred in the Gila and Ma Ha Tuak ranges of South Mountain. The base image is used following permission guidelines for Google Earth.

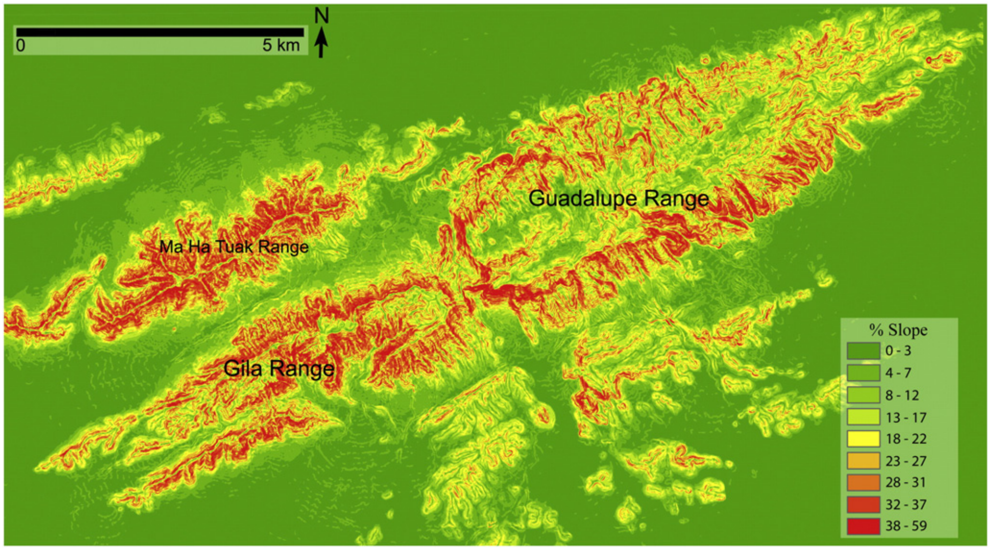


**Fig. 3.** Debris-flow chutes and levees occur on the steepest slopes of the Ma Ha Tuak and Gila ranges of South Mountain that experienced debris flows in 2014.

less (Flood Control District of Maricopa County, 2014b) with the greatest being 36 mm in 25 min (87 mm/h). Another 68 mm then soaked the range over the next 285 min (14 mm/h) where precipitation intensities occasionally exceeded 30 mm/h, but only for 5 min at a time.

## 4. Methods

### 4.1. Field observations

Field surveys after the 12 August and 8 September 2014 events involved the identification of debris-flow chutes and deposits. Debris flows were distinguished from shallow landslides on the basis of such features as levees, lobes, and boulder trains. These surveys involved traversing the crests, slopes and perimeters of the Guadalupe, Ma Ha Tuak, and Gila ranges after both events.

### 4.2. Age estimation of paleodebris flows by varnish microlaminations

Cosmogenic nuclide dating has become a generally preferred geomorphic dating method (Phillips et al., 2016). However, cosmogenic nuclides can experience problems associated with the prior exposure histories of clasts transported from desert slopes to positions on alluvial fans (Nishiizumi et al., 1993; Duhnforth et al., 2007; Frankel et al., 2007a, 2007b; Oskin et al., 2007; Machette et al., 2008; Owen et al., 2011; Fenton and Pelletier, 2013; Ivy-Ochs et al., 2013). In the South Mountain field setting, each debris flow clast could potentially experience a different history of (i) exposure prior to bedrock detachment, (ii) exposure in the upper meter as colluvium, (iii) exposure in the debris-flow chute, and (iv) exposure in a debris-flow levee. Conventional radiocarbon dating suffers in this context from the poor preservation of organic matter in debris-flow matrixes older than a few hundred years. Thus, all debris-flow levees were sampled for VML dating from each of the catchments and run outs that experienced 2014 debris flows. Because varnish forms on top of debris flow boulders, VML can only provide a minimum age.

Climatic events are recorded in micron-scale laminations of rock varnish. Developed by Tanzhuo Liu, VML dating employs a variety of established ages for geomorphic surfaces to produce a region calibration (Liu and Broecker, 2007, 2008, 2013). Additional late Holocene radiocarbon ages on Paloverde wood crushed by rock fall boulders in central Arizona added to this calibration (Dorn, 2014). The method has been subjected to blind testing (Marston, 2003) and has been replicated in different settings (Diaz et al., 2002; Lee and Bland, 2003; Dietzel et al., 2008; Zerboni, 2008; Baied and Somonte, 2013). Sampling procedures and followed guidelines are outlined elsewhere (Liu and Broecker, 2007, 2008, 2013). Additional details on VML dating and sampling issues related to South Mountain are presented in the supplemental file Appendix B.

### 4.3. Strontium isotopes to assess nature of fine matrix

Strontium isotopes have the potential to discriminate source materials (Capo et al., 1998; Capo and Chadwick, 1999) — in this project the origin of the matrix of the debris flows at South Mountain. Debris-flow research in wet environments appropriately assumes that the matrix derives from mineral decay of the host bedrock, producing soil that is then mobilized. An alternative possibility in the Sonoran Desert is that the dust that deposits on slopes in central Arizona (Péwé et al., 1981) could also supply the matrix fines. Figs. 8–10 in Moore et al. (2012) present ten VML ages for debris flow surfaces on the Ma Ha Tuak 1, 2, and 3 fans. After digging 0.5 m into the matrix of debris-flow deposits on these 10 surfaces, fines were collected and were separated into (i) the acetic acid-soluble fraction that represents carbonate and labile Ca, and (ii) the silicate fraction. In addition to the collection of fines, ten gneiss clasts were pulverized and then amalgamated into a composite sample for comparison. Samples were analyzed with a Nuclide 1290 mass spectrometer and results were normalized to the $^{87}Sr/^{86}Sr$ ratio of 0.1194 and compared to the Eimer and Amend NBS987 standard (0.7080; Deines et al., 2003).

## 5. Results

### 5.1. Field observations of debris flows

Table 1 and Fig. 4 present the location, run out length, slope at the point of failure, and the storm that generated each of the 35 debris flows that occurred during the summer of 2014 at South Mountain. In an example of a single debris flow, Fig. 5 presents different views of the Ranger 2 debris-flow chute and deposit. Debris flows initiated at a variety of slope angles were measured at the site of failure with an inclinometer and located with a dGPS system (Table 1). A supplemental KMZ file (Appendix A) allows readers to explore each failure. It may be that a detailed analysis of radar data — which is beyond the scope of this study — might reveal differences in rainfall intensity and duration between slopes that failed and those that did not.

**Table 1**
Debris-flow failures in 2014 at South Mountain, Phoenix; flow names relate to local place names and correspond with the supplemental KMZ file (Appendix A).

| Flow name | Storm | Initiation | Site | Run out length (m) | Slope at failure |
|---|---|---|---|---|---|
| 2014_Ranger1 | 12 August | 33.328320° | −112.089290° | 223 | 46° |
| 2014_Ranger2 | 12 August | 33.327824° | −112.090882° | 635 | 55° |
| 2014_Ranger3 | 12 August | 33.327898° | −112.091631° | 629 | 44° |
| 2014_Ranger4 | 12 August | 33.328119° | −112.094065° | 430 | 43° |
| 2014_MaxDelta1 | 12 August | 33.326638° | −112.094318° | 524 | 53° |
| 2014_MaxDelta2 | 12 August | 33.325843° | −112.095265° | 514 | 51° |
| 2014_MaxDelta3 | 12 August | 33.325666° | −112.097655° | 190 | 44° |
| 2014_MaxDelta4 | 12 August | 33.326113° | −112.097510° | 418 | 48° |
| 2014_MaxDelta5 | 12 August | 33.325693° | −112.098133° | 494 | 57° |
| 2014_National1 | 12 August | 33.326716° | −112.092556° | 243 | 48° |
| 2014_Laveen1 | 12 August | 33.324086° | −112.159672° | 549 | 42° |
| 2014_Laveen2 | 12 August | 33.344476° | −112.161050° | 295 | 20° |
| 2014_Laveen3 | 12 August | 33.323188° | −112.156549° | 568 | 39° |
| 2014_Laveen4 | 12 August | 33.323237° | −112.157336° | 581 | 41° |
| 2014_Laveen5 | 12 August | 33.329308° | −112.149653° | 330 | 50° |
| 2014_SanJuan1 | 12 August | 33.323737° | −112.153689° | 127 | 42° |
| 2014_SanJuan2 | 12 August | 33.325217° | −112.142403° | 499 | 47° |
| 2014_SanJuan3 | 12 August | 33.324191° | −112.142410° | 485 | 41° |
| 2014_SanJuan4 | 12 August | 33.323644° | −112.141050° | 599 | 44° |
| 2014_Elliot1 | 12 August | 33.341729° | −112.110432° | 357 | 59° |
| 2014_Elliot2 | 12 August | 33.341608° | −112.107588° | 441 | 45° |
| 2014_Elliot3 | 12 August | 33.341749° | −112.110080° | 371 | 46° |
| 2014_Elliot4 | 8 September | 33.344628° | −112.111249° | 582 | 14° |
| 2014_Elliot5 | 12 August | 33.334749° | −112.120063° | 261 | 47° |
| 2014_Elliot6 | 8 September | 33.341974° | −112.115253° | 352 | 11° |
| 2014_Elliot7 | 12 August | 33.343328° | −112.106178° | 877 | 40° |
| 2014_19th1 | 8 September | 33.342316° | −112.103838° | 485 | 39° |
| 2014_19th2 | 8 September | 33.342037° | −112.104854° | 532 | 44° |
| 2014_MaHaTuak1 | 12 August | 33.342300° | −112.098930° | 224 | 49° |
| 2014_MaHaTuak2 | 12 August | 33.341278° | −112.102417° | 479 | 32° |
| 2014_MaHaTuak3 | 12 August | 33.341124° | −112.102287° | 440 | 44° |
| 2014_MaHaTuak4 | 12 August | 33.342236° | −112.101724° | 118 | 41° |
| 2014_MaHaTuak5 | 12 August | 33.340778° | −112.106541° | 479 | 50° |
| 2014_MaHaTuak6 | 12 August | 33.331030° | −112.126654° | 339 | 52° |
| 2015_MaHaTuak7 | 12 August | 33.325451° | −112.137625° | 486 | 42° |

Field observations distinguished debris-flow deposits from shallow landslides. From a distance, debris-flow chutes can look superficially similar to a linear shallow landslide failure. Upon closer inspection, shallow landslides lack debris-flow deposits. Over 60 shallow landslides occurred in response to the 12 August 2014 and 8 September 2014 storms. A report on these failures is beyond the scope of this research.

The 8 September event resulted in substantial flooding in adjacent neighborhoods of South Phoenix and Laveen (Flood Control District of Maricopa County, 2014b). The debris-flow chutes that were cleaned out by the 12 August event acted as a more efficient conduit for water transfer, and the second 8 September event was able to remobilize some of 12 August debris flow deposits.

The debris-flow chutes cleaned out by the 12 August event also enabled a firehose effect in some locations of concentrating water at a particular spot (Coe et al., 2008) to generate two 8 September debris flows. Elliot debris flows 1–3 (Fig. 6A) occurred on 12 August. These flows failed on slopes ranging from 45° to 59° with run outs ranging between 357 and 441 m. Much older debris flow deposits at the head of an alluvial fan were saturated by 12 August precipitation and stream flow (Fig. 6B). Then, on 8 September, the cleaned-out chutes of Elliot flows 1–3, as well as cleaned-out tributary washes, funneled water rapidly toward saturated ancient debris-flow deposits. This fire hose effect resulted in an 8 September debris flow (Fig. 6C) that had a run out of 582 m and came within 40 m of a house structure. The Elliot6 debris flow was also generated by a firehose effect on 8 September, when floodwaters destabilized older fanglomerate and generated a 352-m flow that ended about 20 m from a house structure.

### 5.2. Age estimation by varnish microlaminations

Table 2 summarizes the VML ages for older debris-flow levees adjacent to the 2014 flows. Fig. 7 portrays typical VML patterns observed on the debris-flow levees. Each VML date is a minimum age for the underlying debris flow. A supplemental file (Appendix B) presents VML thin section results of debris-flow ages summarized in Table 2.

An important limitation exists in the deployment of VML as a dating technique in the Sonoran Desert. As detailed in previous research (Dorn, 2010, 2014), microcolonial fungi growing on varnish surfaces secrete

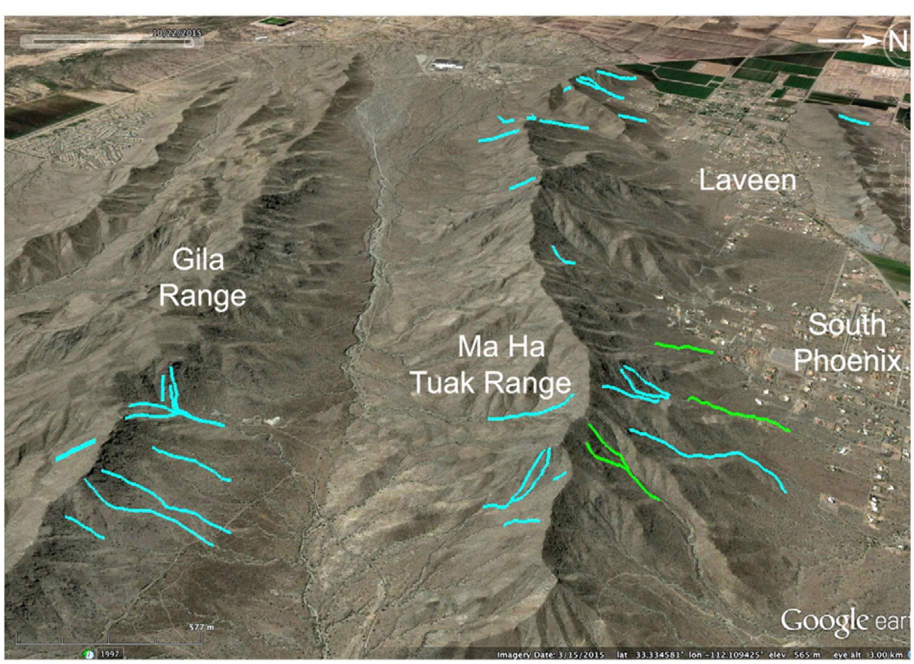


**Fig. 4.** West-looking view of the western ranges of South Mountain showing debris flows of 2014. Lines indicate the debris-flow chutes and run outs that mobilized in the 12 August (blue) and 8 September (green) 2014 summer monsoon events, shown in this west-looking Google Earth view. The Laveen Village and South Phoenix neighborhoods were impacted heavily by flooding. A supplemental KMZ file (Appendix A) allows exploration of each of the debris-flow paths.

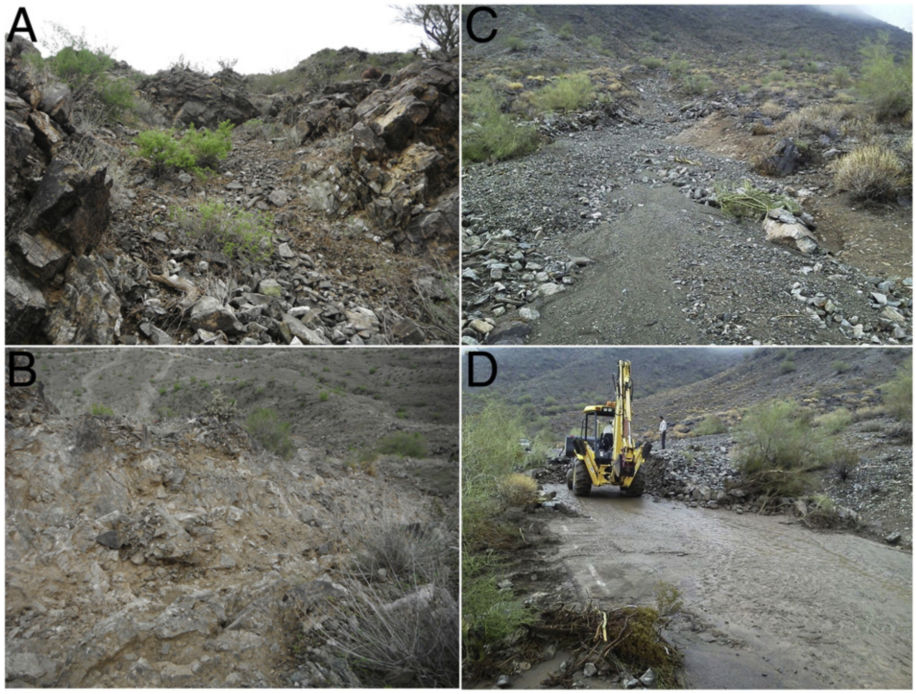


**Fig. 5.** Ranger 2 debris-flow chute looking up at the location of initial failure (A) and looking down at the cleaned out chute (B). The debris-flow deposit (C, D) displayed thicknesses between 1 and 3.5 m.

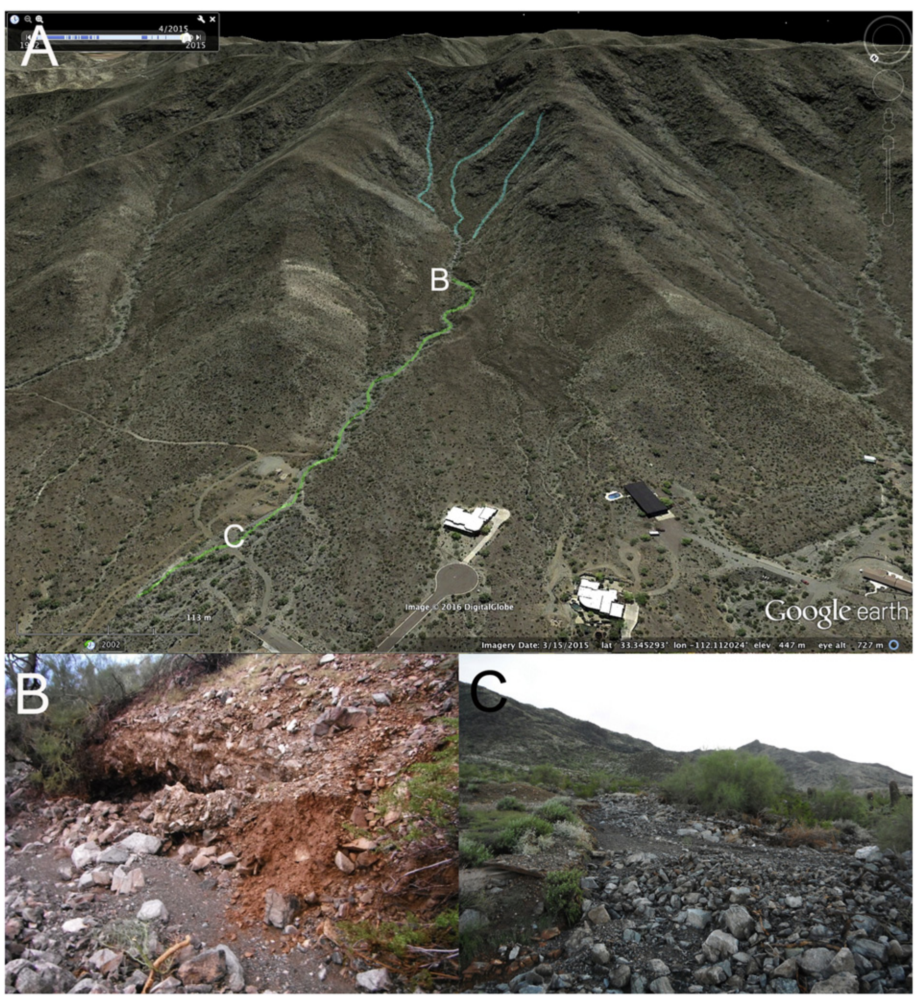


**Fig. 6.** Debris flows near Elliot Drive, Phoenix, failed in two different storms. (A) Blue lines denote Elliot flows 1-3 (Table 1) that failed 12 August, while the green line indicates Elliot flow 4 that failed 8 September. (B) Photograph taken August 12 of saturated bank composed of late Pleistocene debris-flow deposits. This bank experienced a firehose effect on 8 September. (C) The 8 September debris-flow deposit generated by the firehose effect of runoff aimed at steep banks of older debris-flow deposits. Locations of the photographs (B) and (C) are indicated in (A).

**Table 2**
VML ages of debris-flow levees adjacent to the 2014 debris-flow failures; flow names are combined into a single row where they are close together.[a]

| VML pattern | <WH1 | WH1 | WH2–3 | WH3 | WH4 | WH9 | WH11 | WP1 | LU3 | WP2 | WP3 |
|---|---|---|---|---|---|---|---|---|---|---|---|
| Calendar age (ka) | <0.35 | 0.3–0.65 | 1.1–1.4 | 1.4 | 2.8 | 8.1 | 10.3 | 16.5 | 16.5–24 | 24 | 30 |
| Individual flows | | | | | | | | | | | |
| 2014_Ranger1 | | | | | X | X | | | | | |
| 2014_Ranger2 | | | | | | X | | X | | | |
| 2014_Ranger3 | | | | | X | X | | X | | | |
| 2014_Ranger4 | X | | | | | X | | X | | | |
| 2014_MaxDelta1-5 | X | X | X | | X | X | | X | X | | |
| 2014_National1 | | X | | | X | | | | | | |
| 2014_Laveen1 | | X | | | | X | X | X | | | |
| 2014_Laveen2-3 | | | | | X | X | | X | | X | |
| 2014_Laveen4 | | | | | X | | | X | | | |
| 2014_Laveen5 | | | | | | X | | X | | X | |
| 2014_SanJuan1 | | X | | | | X | | | | X | |
| 2014_SanJuan2 | | | | | X | X | | | | | |
| 2014_SanJuan3 | | X | | | X | X | X | | | | |
| 2014_SanJuan4 | X | X | X | | X | | | | | | |
| 2014_Elliot1-4 | | X | | | | | | X | X | | |
| 2014_Elliot5 | X | | | | X | X | | X | X | | |
| 2014_Elliot6 | | X | | | X | | | X | | | X |
| 2014_Elliot7 | X | | X | | | | | | X | | |
| 2014_19th1-2 | | X | | X | X | X | X | X | | X | |
| 2014_MaHaTuak1 | | | X | | X | | | | | | |
| 2014_MaHaTuak2-4 | | | | X | | | | | | | |
| 2014_MaHaTuak5 | | X | | | X | | | | | | |
| 2014_MaHaTuak6 | X | X | | | X | | | | | | |
| 2014_MaHaTuak7 | | X | | | X | | | | | | |

[a] The W, WP, and LU3 abbreviations refer to Wet Holocene black layers, Wet Pleistocene black layers, and Layering Unit 3 nomenclature employed by Liu and Broecker (2007, 2008, 2013). Reported age ranges are based on multiple calibrations by Liu and Broecker (2007, 2008, 2013). A supplemental file (Appendix B) presents VML analyses from all of the debris-flow deposits indicated in this table.

acids that dissolve the varnish microstratigraphy in places. While careful sample selection in the field can avoid obvious growths, detection is difficult when varnish covers over these organisms. The problem of VML pattern loss from these organisms means that only 20% of the sampled flows are presented in Table 2 (and the supplemental file Appendix B). This is because microcolonial fungi disrupted the VML pattern in about 80% of the samples.

With these limitations, a few findings are evident from the results summarized in Table 2. First, sampling within a single small drainage provides only limited insight into the minimum frequency of debris flows within a desert mountain range. Some drainage areas have a geometry that allows debris flows to spread out and facilitate preservation of older flows, while other drainages funnel flows through the same narrow corridor that results in the erasure of older levees by more recent events. Second, considering only the basins that experienced debris flows in 2014, 74% of these basins contain evidence of prior debris flows in the last 650 years. Third, debris flows ~2.8, ~8.1, and ~16.5 ka deposited extensive levees, at least enough to survive erasure by subsequent debris flows.

### *5.3. Strontium isotopes to assess nature of fine matrix*

Samples collected from debris flow matrixes within different aged surfaces of three alluvial fans previously mapped from the Ma Ha Tuak range (Moore et al., 2012) have $^{87}Sr/^{86}Sr$ ratios of ~0.71 (Table 3). In contrast, the gneissic clasts in these debris flows have substantially different $^{87}Sr/^{86}Sr$ ratios of ~0.73.

## 6. Discussion

### *6.1. South Mountain case study supports hazard approach in warm desert setting*

A debris-flow hazard analysis starts with recognition for the potential for a debris flow, followed by a probability analysis (Jakob, 2005). Based on varnish microlamination dating, minimum ages for debris-flow deposits (Dorn, 2010) revealed that debris flows could be a hazard for homes located next to the small mountain ranges of Phoenix, AZ (Dorn, 2012). The debris flows that occurred at South Mountain in the summer of 2014 (Table 1) were, therefore, predictable and predicted.

A global database (Guzzetti et al., 2008) sorts debris flow events using the Köppen climate classification. In this classification system, South Mountain falls in the Bwh Köppen designation for an arid hot climate. Using this global database (Guzzetti et al., 2008), plotting of peak intensity and duration of precipitation reveals the 12 August and 8 September 2014, events to be on the upper end for desert climates (Fig. 8). Thus, from a global perspective, debris-flow generation would also be expected in Phoenix, AZ, at even lower precipitation intensities.

An implication of the predicted occurrence (Table 1) and the potential for future debris-flow occurrence at lower rainfall intensities (Fig. 8) is that the next steps of a debris-flow hazard analysis are now warranted for the Phoenix, AZ, area adjacent to steep mountain slopes. The next steps involve estimating debris-flow magnitude and intensity, documenting frequency-magnitude relationships, and mapping the full extent of hazards (Jakob, 2005).

### *6.2. A new perspective on re-arming debris-flow chutes in deserts*

A dominant paradigm in the southwestern USA demands a wetter climate to re-arm debris-flow chutes with fines and larger clasts. This model derives from early twentieth century observations (Huntington, 1907) followed by others (Bull and Schick, 1979; Mayer et al., 1984; Wells et al., 1984; Bull, 1991; Harvey and Wells, 1994) who maintained the perspective that soil and colluvium production occurred predominantly during wetter glacial periods. Then, during the drier Holocene, soils were eroded over time from slopes and transported to alluvial fans.

The evidence obtained from VML studies of debris-flow levees at South Mountain suggests that a mechanism exists to re-arm slopes — including debris-flow chutes — during the Holocene with fine and coarse materials. Prior data (Dorn, 2010) and the new VML results presented here (Table 2) provide empirical evidence that re-arming must have occurred throughout the Holocene. Two processes could explain

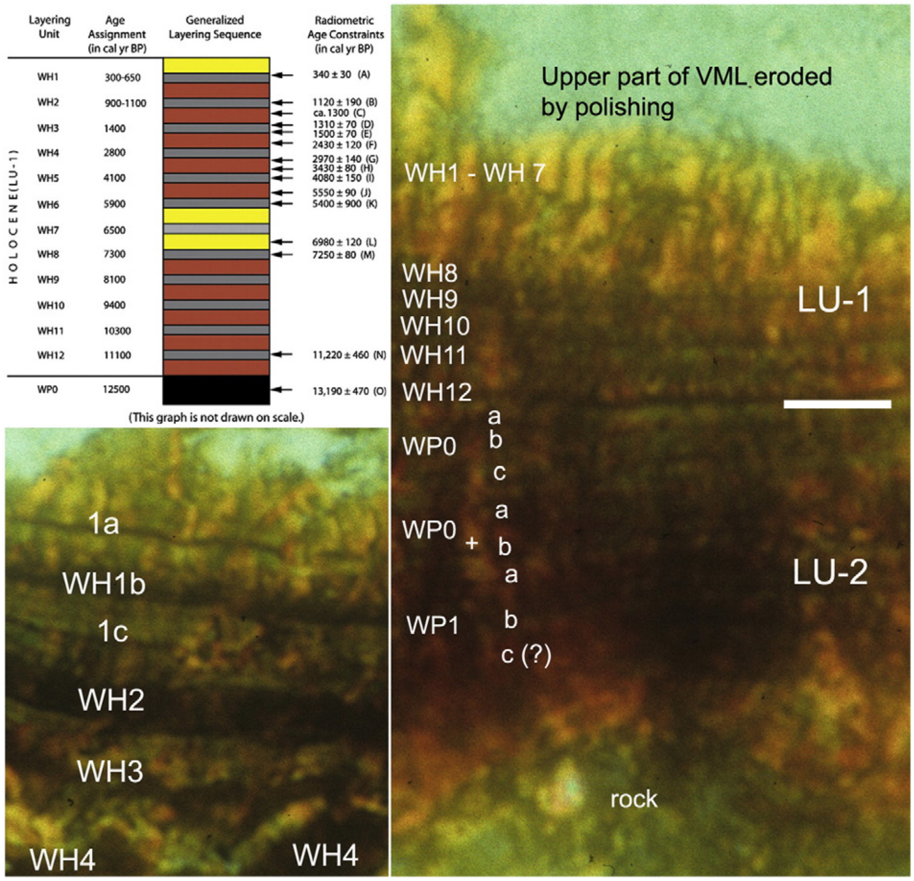


**Fig. 7.** Typical VML patterns for varnishes on debris-flow levees — in this figure collected from the Elliot basins (see Table 2). The VML nomenclature indicates black Wet Holocene (WH) layers and Wet Pleistocene (WP) laminations. The Holocene calibration graphic is from Liu and Broecker (2007). A supplemental file (Appendix B) presents VML analyses from the debris-flow deposits indicated in Table 2.

the ample supply of fine and coarse material in debris-flow chutes throughout the Holocene: dust deposition and dirt cracking.

Dust deposition occurs regularly in association with Arizona summer monsoon season (Péwé et al., 1981; Marcus and Brazel, 1992). The $^{87}Sr/^{86}Sr$ ratios indicated previously that the fine material being moved in overland flow as suspended load at South Mountain is derived from this dust (Dorn, 2015). The $^{87}Sr/^{86}Sr$ ratio of ~0.71 for fines in debris-flow matrixes (Table 3) is also consistent with prior research on $^{87}Sr/^{86}Sr$ ratios in desert dust (Capo et al., 1998; Stewart et al., 1998; Capo and Chadwick, 1999; Naiman et al., 2000) and also the carbonate derived from desert dust (Harrison and Dorn, 2014).

The $^{87}Sr/^{86}Sr$ ratios for debris-flow matrixes differ substantially from prior $^{87}Sr/^{86}Sr$ analyses of South Mountain material derived from the source rocks (Dorn, 2015) and differ substantially from the gneissic clasts collected next to the fines in debris-flow matrixes (Table 3). Thus, the fines needed to mobilize debris flows appear to derive from desert dust deposition and not *in situ* mineral decay. Therefore, the rate of dust deposition, not the rate of rock decay, is the limiting factor on re-arming debris-flow chutes with fines. Unfortunately, rates of natural dust deposition in the Sonoran Desert are not available, and contemporary dust deposition rates are greatly impacted by human activity.

A second process that re-arms debris-flow chutes is the production of gravel, cobbles, and boulders. The process of dirt cracking (Dorn, 2011) provides the physical mechanism to resupply boulders and cobble clasts to debris-flow chutes. Dirt cracking starts with the growth of laminar calcrete in narrow fractures, opening up enough space for dust penetration — creating a positive feedback where each increment of fracture deepening and widening permits more laminar calcrete and dust penetration. This process continues until detachment occurs. Dirt cracking does not require a wetter climate to operate, and some evidence suggests that dirt cracking is more efficient in drier conditions in central Arizona (Dorn, 2014). Thus, present-day conditions in the Sonoran Desert — and perhaps other desert regions with an abundant supply of dust — permit the resupply of fines and clasts (Fig. 9). There is no reason, therefore, to invoke the need for climate change on desert slopes or to conclude that debris flows are mining fossil materials produced under a different climate.

### 6.3. The next steps in a hazard analysis

Some progress has been made on the first two steps in a debris-flow hazard analysis. Debris flow deposits occur widely on slopes and debris-flow fans that exit from debris-flow chutes in small ranges abutting homes in Phoenix, AZ (Dorn, 2010, 2012; Moore et al., 2012). Using exposed debris-flow levees, a probability analysis for the northern Ma Ha Tuak Range revealed a minimum occurrence of 5 debris flows per century in the last 8100 years (Dorn, 2010). The 118–877 m range of run out lengths of 2014 debris flows at South Mountain (Table 1) yield some insight into the magnitude associated with two different types of summer precipitation events: thunderstorm and hurricane moisture. Furthermore, a debris flow that occurred in January 2010 on the northern fringes of Phoenix (Dorn, 2010) indicates that winter precipitation from frontal storm can also generate debris flows in the area.

In Arizona, USA, flood control districts exist as a political subdivision overseen by a County Board of Supervisors and receiving counsel from an advisory board comprised of county citizens. The Flood Control District of Maricopa County is the agency responsible for the unincorporated areas around Phoenix, AZ, while the City retains the flood control authority within city limits. Flood control planning and hazard

**Table 3**
$^{87}Sr/^{86}Sr$ analyses from debris flows collected at South Mountain.[a]

| Fan | VML Calendar Age | $^{87}Sr/^{86}Sr$ ratio Fines HCl leachate | $^{87}Sr/^{86}Sr$ ratio Fines silicate fraction | $^{87}Sr/^{86}Sr$ ratio Gneiss clasts HCl leachate |
|---|---|---|---|---|
| Ma Ha Tuak 1 | 0.3–0.65 ka | 0.7080 | 0.7116 | 0.7322 |
| | 1.4–0.9 ka | 0.7078 | 0.7119 | 0.7254 |
| | 24–16.5 ka | 0.7079 | 0.7108 | 0.7277 |
| Ma Ha Tuak 2 | 0.3–0.65 ka | 0.7076 | 0.7112 | 0.7283 |
| | 16.5 ka | 0.7080 | 0.7115 | 0.7308 |
| | 24–16.5 ka | 0.7088 | 0.7114 | 0.7310 |
| Ma Ha Tuak 3 | 0.3–0.65 ka | 0.7068 | 0.7113 | 0.7260 |
| | 2.8 ka | 0.7070 | 0.7105 | 0.7253 |
| | 16.5 ka | 0.7070 | 0.7121 | 0.7300 |
| | 30 ka | 0.7083 | 0.7122 | 0.7289 |

[a] The debris flows are mapped in Figs. 8–10 in Moore et al. (2012) for the Ma Ha Tuak fans 1, 2, and 3; reported age ranges are based on multiple calibrations for varnish microlaminations by Liu and Broecker (2007, 2008, 2013).

delineation is funded by a property tax. The Flood Control District of Maricopa County and the City of Phoenix have the responsibility to carry out the remaining steps of a debris flow hazard analysis for several reasons.

First, Title 44 of The Code of Federal Regulations (Emergency Management and Assistance), Chapter 1 (Federal Emergency Management Agency, Department of Homeland Security) Chapter 1, Subchapter B, Part 65.13 specifies:

> '(c) FEMA will credit on NFIP (National Flood Insurance Program) maps [where]… The potential for debris flow and sediment movement must be assessed using an engineering method acceptable to FEMA. The assessment should consider the characteristics and availability of sediment in the drainage basin above the apex and on the alluvial fan.'

The debris flows adjacent to current and planned home sites on alluvial fans certainly qualify under the assessment that must be carried out to generate the NFIP maps required of the MCFCD. Three mechanisms can generate debris flows of sufficient length and magnitude to reach homes: (i) intense precipitation such as occurred on 12 August 2014; (ii) a firehose effect of concentrated runoff (Fig. 10) such as occurred on 8 September 2014; and (iii) soaking frontal winter precipitation (Dorn, 2010).

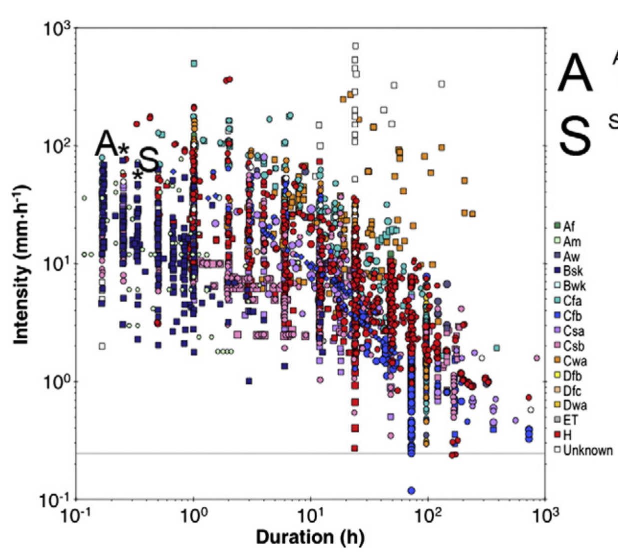


**Fig. 8.** Worldwide rainfall intensity and duration conditions resulting in debris flows and shallow landslides plotted by Köppen climate classification (Guzzetti et al., 2008). Each site in a given Köppen climate type is plotted where precipitation intensities and duration are known. B-type climates are considered arid. Peak intensities for the South Mountain debris flow events are superimposed on the global data base with positions shown by asterisks next to the 12 August (A) and 8 September (S) 2014 events.

Second, the cleaned-out chutes generated by debris flows significantly alter characteristics of overland flow derived from these mountain slopes. The 8 September 2014 rain event created a firehose effect (Coe et al., 2008) that then contributed debris-flow generation from older alluvial-fan deposits (Fig. 6) and also to the flooding experienced in the nearby Phoenix neighborhood of Laveen that rests in part on alluvial fans (Flood Control District of Maricopa County, 2014b).

Third, it is the author's opinion that there MCFCD has an ethical responsibility to the existing and future homeowners in central Phoenix who have debris-flow chutes above their homes. When they purchased their homes, these chutes were not viewed as a hazard (Harris and Pearthree, 2002). With the 2014 validation (Table 1) of an analysis of past debris-flow occurrences in a Phoenix mountain range (Dorn, 2010), Phoenix and Flood Control District of Maricopa County now need to identify the houses downslope of debris-flow chutes in the central portion of Phoenix, AZ. Although homeowners in the older portion of Phoenix have been paying taxes to the MCFCD, most of these projects occur on the periphery as the Phoenix area continues to expand. An unknown number of homeowners in the urban center now have clearly recognized debris flow hazard. The 2014 debris flows at South Mountain highlight the need for the Flood Control District of Maricopa County to complete a formal hazards analysis at the full urban-mountain interface.

## 7. Conclusion

Debris flows help build alluvial fans in desert regions (Blair and McPherson, 2009), generated by intense and short duration precipitation events (Guzzetti et al., 2008). With notable exceptions (Moreiras, 2006; Sepulveda et al., 2006; Webb et al., 2013; Shaw, 2015; Stolle et al., 2015; Zhou et al., 2016), however, debris flows are not generally considered a hazard to urban infrastructure in warm desert settings like Phoenix, AZ.

This general perception that debris flows do not pose a hazard to cities that abut small mountains in warm deserts is in need of revision. Following basic guidelines in the identification of debris-flow hazards (Jakob, 2005), VML dating established that at least 5 debris flows per century occurred on the north side of a small mountain range abutting neighborhoods in south Phoenix, Arizona (Dorn, 2010). The existence of a hazardous condition was then confirmed dramatically in the summer of 2014 when two different rainstorms generated 35 debris flows in this same study area previously analyzed by VML dating. Two different processes generated debris flows in 2014: intense precipitation on steep slopes and a firehose effect where runoff mobilized older debris-flow deposits. In 2010 a third process generated a debris flow on the northern fringe of Phoenix: frontal winter precipitation soaking a desert slope over a few days (Dorn, 2010).

Arguments that desert debris flows have very slow rates of resupply owing to slow rates of soil production in dry climates do not apply in settings like the Sonoran Desert with abundant dust storms. The $^{87}Sr/^{86}Sr$ analysis of fines in South Mountain debris flows of different

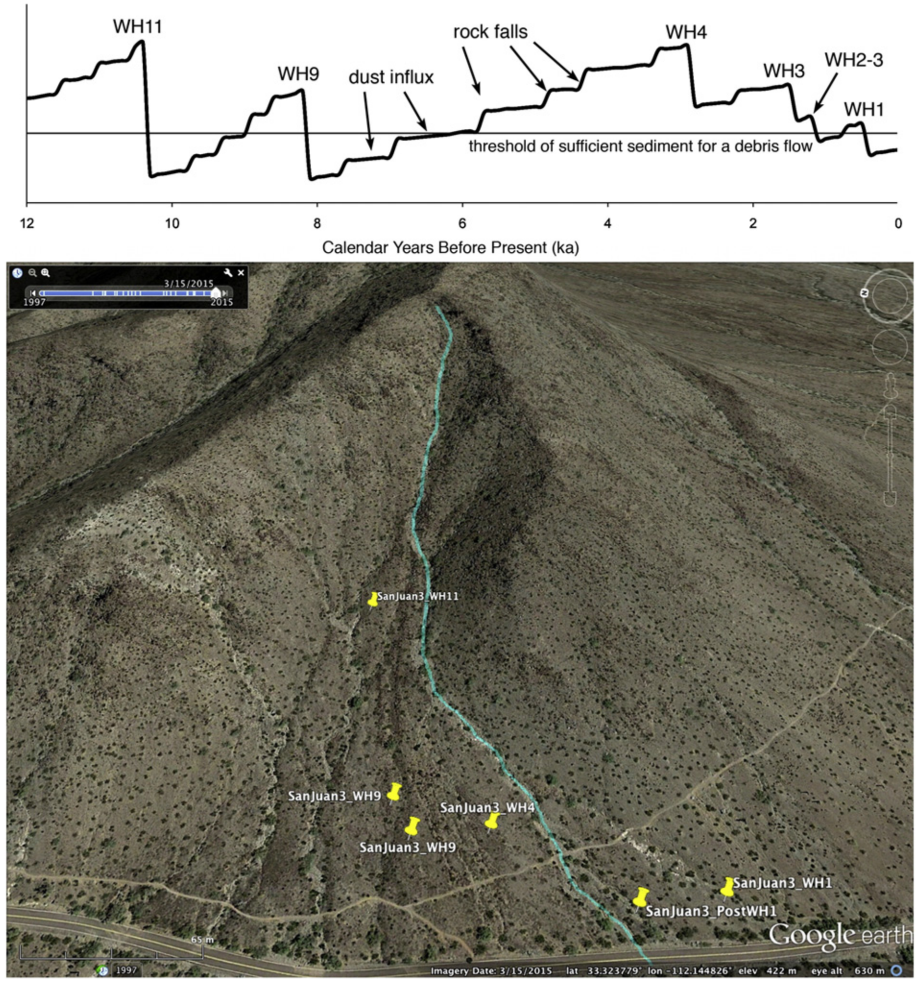


**Fig. 9.** A conceptual model for debris-flow chute rearming under present-day conditions in the Sonoran Desert, where the vertical axis in the graph indicates the amount of colluvium and fines accumulated in a debris-flow chute. The conceptual graph also refers to specific VML ages for debris-flow levees sampled adjacent to the San Juan 2014 debris flow indicated by the line. Pins indicate the sampling location for debris-flow levees of various Holocene ages (Table 2). The model of re-arming desert slopes without climatic change is only conceptual because rates of dust influx, rates of rock fall influx, and threshold of sufficient sediment to generate a debris flow are unknown at present.

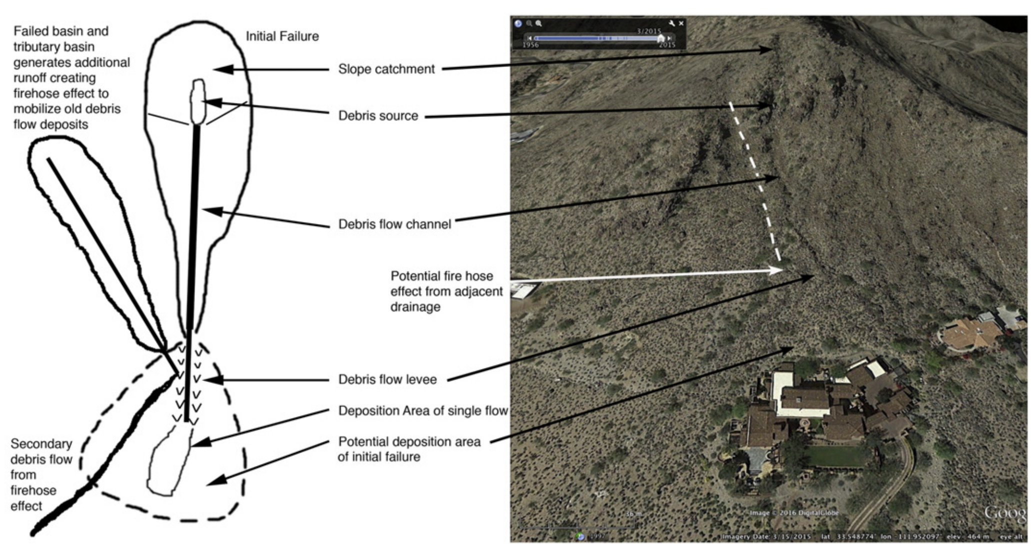


**Fig 10.** Idealized concept of debris-flow generation by two different processes in small arid basins of the Sonoran Desert. Field observations from the 2014 debris flow events at South Mountain indicate that failures high up on the steeper slopes of small drainages (Initial Failure) occur from high intensity precipitation events. This initial failure and also erosion associated with flooding in a tributary basin can set up conditions for subsequent debris flows from a firehose effect. The cleaned-out debris-flow chutes and tributary channels can end up funneling water efficiently to older debris-flow deposits. This process could potentially occur above home sites like this one. Mobilization of these older deposits can allow debris flows to extend farther down the piedmont than initial failures — as seen for the Elliot4 (Fig. 6) and Elliot6 debris flows on 8 September (Table 2).

ages reveals that desert dust supplies fines, whereas the gneissic boulders in the flows have a different $^{87}Sr/^{86}Sr$ signature. Larger clasts are resupplied to debris-flow chutes by dirt cracking (Dorn, 2011). Rates of dust deposition, thus, limit debris-flow re-arming in the Sonoran Desert and perhaps other deserts with frequent dust storms (Goudie and Middleton, 2006).

The results presented here attest to the power of VML dating as a technique (Liu, 2016) to provide minimum ages for the abrasion of rock surfaces in deserts because these VML results led to the accurate prediction that debris flows pose a hazard for homes built underneath desert slopes in the Sonoran Desert of North America.

## Acknowledgements

The author thanks the Phoenix Parks and Recreation Department for permission to collect samples for analysis, Tanzhuo Liu for permission to use his VML calibration graphic and Fauso Guzzetti for permission to use his graphic compiling debris flows based on intensity-duration data for different Köppen climates. Two anonymous reviewers and editor Dr. Richard Marston made suggestions that greatly improved the manuscript.

Maps. Debris flows that occurred at South Mountain, Phoenix, Arizona, in 2014.

## Appendix A. Supplementary data

Supplementary data associated with this article can be found in the online version, at doi: http://dx.doi.org/10.1016/j.geomorph.2016.08.013 where data consist of varnish microlamination images annotated to highlight the layering patterns identified in Table 2. The imagery is preceded by text providing supplemental information on the interpretation of the patterns used to date varnish accretion. These data also consist of a Google KMZ file showing the 2014 debris flow run outs at South Mountain, Sonoran Desert, USA.

## References

Arnáez, J., Lana-Renault, N., Lasanta, T., Ruiz-Flaño, P., Castroviejo, J., 2015. Effects of farming terraces on hydrological and geomorphological processes. A review. Catena 128, 122–134.

Baied, C.A., Somonte, C., 2013. Mid-Holocene geochronology, palaeoenvironments, and occupational dynamics at Quebrada de Amaicha, Tucuman, Argentina. Quat. Int. 299, 80–89.

Beaumont, P., 1972. Alluvial fans along the foothills of the Elburz Mountains, Iran. Palaeogeogr. Palaeoclimatol. Palaeoecol. 12, 251–273.

Blair, T.C., McPherson, J.G., 2009. Processes and forms of alluvial fans. In: Parsons, A.J., Abrahams, A.D. (Eds.), Geomorphology of Desert Environments, 2nd ed. Springer, Amsterdam, pp. 413–467.

Bull, W.B., 1991. Geomorphic Responses to Climatic Change. Oxford University Press, Oxford.

Bull, W.B., Schick, A.P., 1979. Impact of climatic change on an arid watershed: Nahal Yael, southern Israel. Quat. Res. 11, 153–171.

Butler, D.R., Malanson, G.P., Oelfke, J.G., 1987. Tree-ring analysis and natural hazard chronologies: minimum sample sizes and index values. Prof. Geogr. 39, 41–47.

Capo, R.C., Chadwick, O.A., 1999. Sources of strontium and calcium in desert soil and calcrete. Earth Planet. Sci. Lett. 170, 61–72.

Capo, R.C., Stewart, B.A., Chadwick, O.A., 1998. Strontium isotopes as tracers of ecosystem processes: theory and methods. Geoderma 82, 197–225.

Coe, J.A., Kinner, D.A., Godt, J.W., 2008. Initiation conditions for debris flows generated by runoff at Chalk Cliffs, central Colorado. Geomorphology 96, 270–297.

Coney, P.J., Harms, T.A., 1984. Cordilleran metamorphic core complexes: Cenozoic extensional relics of Mesozoic compression. Geology 12, 550–554.

De Paola, F., De Risi, R., Di Crescenzo, G., Giugni, M., Santo, A., Speranza, G., 2015. Probabilistic assessment of debris flow peak discharge by Monte Carlo simulation. ASCE-ASME J. Risk Uncertain. Eng. Syst. A Civil Eng., A4015002 http://dx.doi.org/10.1061/AJRUA6.0000855.

Deines, P., Goldstein, S.L., Oelkers, E.H., Rudnick, R.L., Walter, L.M., 2003. Standards for publication of isotope ratio and chemical data in chemical geology. Chem. Geol. 202, 1–4.

Diaz, T.A., Bailley, T.L., Orndorff, R.L., 2002. SEM analysis of vertical and lateral variations in desert varnish chemistry from the Lahontan Mountains, Nevada. Geological Society of America Abstracts with Programs May 7–9 Meeting <///gsa.confex.com/gsa/2002RM/finalprogram/abstract_33974.htm>.

Dietrich, A., Krautblatter, M., 2016. Evidence for enhanced debris-flow activity in the Northern Calcareous Alps since the 1980s (Plansee, Austria). Geomorphology http://dx.doi.org/10.1016/j.geomorph.2016.01.013.

Dietzel, M., Kolmer, H., Polt, P., Simic, S., 2008. Desert varnish and petroglyphs on sandstone — geochemical composition and climate changes from Pleistocene to Holocene (Libya). Chem. Erde 68, 31–43.

Dorn, R.I., 2010. Debris flows from small catchments of the Ma Ha Tuak Range, Metropolitan Phoenix, Arizona. Geomorphology 120, 339–352.

Dorn, R.I., 2011. Revisiting dirt cracking as a physical weathering process in warm deserts. Geomorphology 135, 129–142.

Dorn, R.I., 2012. Do debris flows pose a hazard to mountain-front property in metropolitan Phoenix, Arizona? Prof. Geogr. 64, 197–210.

Dorn, R.I., 2014. Chronology of rock falls and slides in a desert mountain range: case study from the Sonoran Desert in south-central Arizona. Geomorphology 223, 81–89.

Dorn, R.I., 2015. Impact of consecutive extreme rainstorm events on particle transport: case study in a Sonoran Desert range, western USA. Geomorphology 250, 53–62.

Duhnforth, M., Ivy-Ochs, S., Densmore, A.L., Kubik, P.W., 2007. Constraints on the timing of fan deposition in Death Valley, California, using cosmogenic 10Be and 26Al. Geol. Soc. Am. Abstr. Programs 39 (6), 260.

Fenton, C.R., Pelletier, J.D., 2013. Cosmogenic 3He age estimates of Plio-Pleistocene alluvial-fan surfaces in the Lower Colorado River Corridor, Arizona, USA. Quat. Res. 79, 86–99.

Flood Control District of Maricopa County, 2014a. Storm Report: August 12, 2014. Vicinity of South Mountain Park - Phoenix, AZ. Maricopa County Flood Control District, Phoenix.

Flood Control District of Maricopa County, 2014b. Storm Report: September 8, 2014. Maricopa County Flood Control District, Phoenix.

Frankel, K.L., Brantley, K.S., Dolan, J.F., Finkel, R.C., Klinger, R.E., Knott, J.R., Machette, M.N., Owen, L.A., Phillips, F.M., Slate, J.L., Wernicke, B., 2007a. Cosmogenic 10Be and 36Cl geochronology of offset alluvial fans along the northern Death Valley fault zone: Implications for transient strain in the eastern California shear zone. J. Geophys. Res. Solid Earth 112. http://dx.doi.org/10.1029/2006JB004350.

Frankel, K.L., Dolan, J.F., Finkel, R.C., Owen, L.A., Hoeft, J.S., 2007b. Spatial variations in slip rate along the Death Valley-Fish Lake Valley fault system determined from LiDAR topographic data and cosmogenic 10Be geochronology. Geophys. Res. Lett. 34. http://dx.doi.org/10.1029/2007GL030549.

Fuchs, M., Reverman, R., Owen, L.A., Frankel, K.L., 2015. Reconstructing the timing of flash floods using 10Be surface exposure dating at Leidy Creek alluvial fan and valley, White Mountains, California–Nevada, USA. Quat. Res. 83, 178–186.

Gartner, J.E., Santi, P.M., Cannon, S.H., 2015. Predicting locations of post-fire debris-flow erosion in the San Gabriel Mountains of southern California. Nat. Hazards Earth Syst. Sci. 77, 1305–1321.

Goudie, A., Middleton, N.J., 2006. Desert Dust in the Global System. Springer, London.

Guzzetti, F., Peruccacci, S., ROssi, M., Start, C.P., 2008. The rainfall intensity–duration control of shallow landslides and debris flows: an update. Landslides 5, 3–17.

Harris, R.C., Pearthree, P.A., 2002. A home buyer's guide to geological hazards in Arizona. Ariz. Geol. Surv. Down-To-Earth 13, 1–36.

Harrison, E.J., Dorn, R.I., 2014. Introducing a terrestrial carbon pool in warm desert bedrock mountains, Southwestern USA. Glob. Biogeochem. Cycles 253–268.

Harvey, A.M., Wells, S.G., 1994. Late Pleistocene and Holocene changes in hillslope sediment supply to alluvial fan systems: Zzyzx, California. In: Millington, A.C., Pye, K. (Eds.), Environmental Change in Drylands: Biogeographical and Geomorphological Perspectives. Wiley & Sons, London, pp. 67–84.

Holt, W.E., Chase, C.G., Wallace, T.C., 1986. Crustal structure from 3-dimensional gravity modeling of a metamorphic core complex - a model for Uplift, Santa Catalina-Rincon Mountains, Arizona. Geology 14 (11), 927–930.

Hooke, R.L., 1967. Processes on arid region alluvial fans. J. Geol. 75, 438–460.

Huntington, E., 1907. Some characteristics of the glacial period in non-glaciated regions. Geol. Soc. Am. Bull. 18, 351–388.

Hürlimann, M., Copons, R., Altimir, J., 2006. Detailed debris flow hazard assessment in Andorra: a multidisciplinary approach. Geomorphology 78, 359–372.

Ivy-Ochs, S., Dühnforth, M., Densmore, A.L., Alfimov, V., 2013. Dating fan deposits with cosmogenic nuclides. In: Schneuwly-Bollschweiler, M., Stoffel, M., F., R.-M. (Eds.), Dating Torrential Processes on Fans and Cones. Springer, Amsterdam, pp. 243–263.

Jakob, M., 2005. Debris-flow hazard analysis. In: Jakob, M., Hungr, O. (Eds.), Debris-Flow Hazards and Related Phenomena. Springer, Berlin, pp. 411–443.

Jakob, M., Hungr, O., 2005. Debris-Flow Hazards and Related Phenomena. Springer, Berlin.

Lee, M.R., Bland, P.A., 2003. Dating climatic change in hot deserts using desert varnish on meteorite finds. Earth Planet. Sci. Lett. 206, 187–198.

Lee, M.J., Park, I., Won, J.S., Lee, S., 2016. Landslide hazard mapping considering rainfall probability in Inje, Korea. Geomatics Nat. Hazards Risk 7, 424–446.

Liu, T., 2016. VML Dating Lab. http://www.vmldating.com (last accessed March 13).

Liu, T., Broecker, W.S., 2007. Holocene rock varnish microstratigraphy and its chronometric application in drylands of western USA. Geomorphology 84, 1–21.

Liu, T., Broecker, W.S., 2008. Rock varnish microlamination dating of late Quaternary geomorphic features in the drylands of the western USA. Geomorphology 93, 501–523.

Liu, T., Broecker, W.S., 2013. Millennial-scale varnish microlamination dating of late Pleistocene geomorphic features in the drylands of western USA. Geomorphology 187, 38–60.

Machette, M.N., Slate, J.L., Phillips, F.M., 2008. Terrestrial cosmogenic-nuclide dating of alluvial fans in Death Valley, California. U.S. Geol. Surv. Prof. Pap. 1755, 1–44.

Marcus, M.G., Brazel, A.J., 1992. Summer dust storms in the Arizona Desert. In: Janelle, D.G. (Ed.), Geographical Snapshots of North America. Guilford Press, New York, pp. 411–415.

Marston, R.A., 2003. Editorial note. Geomorphology 53, 197.

Mayer, L., Gerson, R., Bull, W.B., 1984. Alluvial gravel production and deposition – a useful indicator of Quaternary climatic changes in deserts (a case study in southwestern Arizona). Catena Suppl. 5, 137–151.
Melton, M.A., 1965. The geomorphic and paleoclimatic significance of alluvial deposits in southern Arizona. J. Geol. 73, 1–38.
Miller, D.J., Burnett, K.M., 2008. A probabilistic model of debris-flow delivery to stream channels, demonstrated for the Coast Range of Oregon, USA. Geomorphology 94, 184–205.
Moore, M.J., Kraetz, G., Dorn, R.I., 2012. Phoenix debris flow hazard assessment: house location matters. Phys. Geogr. 33, 491–513.
Moreiras, S.M., 2006. Frequency of debris flows and rockfall along the Mendoza river valley (Central Andes), Argentina: associated risk and future scenario. Quat. Int. 158, 110–121.
Naiman, Z., Quade, J., Patchett, P.J., 2000. Isotopic evidence for eolian recycling of pedogenic carbonate and variations in carbonate dust sources throughout the southwestern United States. Geochim. Cosmochim. Acta 64, 3099–3109.
Nations, D., Stump, E., 1981. Geology of Arizona. Kendall Hunt, Dubuque.
Nishiizumi, K., Kohl, C., Arnold, J., Dorn, R., Klein, J., Fink, D., Middleton, R., Lal, D., 1993. Role of in situ cosmogenic nuclides $^{10}$Be and $^{26}$Al in the study of diverse geomorphic processes. Earth Surf. Process. Landf. 18, 407–425.
Oskin, M., Perg, L., Blumentritt, D., Mukhopadhyay, S., Iriondo, A., 2007. Slip rate of the Calico fault: implications for geologic versus geodetic rate discrepancy in the Eastern California Shear Zone. J. Geophys. Res. 112. http://dx.doi.org/10.1029/2006JB004451.
Owen, L.A., Frankel, K., Knott, J.R., Reynhout, S., Finkel, R.C., Dolan, J.F., Lee, J., 2011. Beryllium-10 terrestrial cosmogenic nuclide surface exposure dating of Quaternary landforms in Death Valley. Geomorphology 125, 541–557.
Pearthree, P.A., Youberg, A., Cook, C.P., 2007. Debris flows; an underappreciated flood (?) hazard in southern Arizona. Geol. Soc. Am. Abstr. Programs 39 (5), 11.
Péwé, T.L., Péwé, R.H., Journaux, A., Slatt, R.M., 1981. Desert dust: characteristics and rates of deposition in central Arizona. Geol. Soc. Am. Spec. Pap. 186, 169–190.
Phillips, F.M., Argento, D.C., Bourlès, D.L., Caffee, M.W., Dunai, T.J., Goehring, B., Gosse, J.C., Hudson, A.M., Kelly, M., Lifton, N., 2016. Where now? Reflections on future directions for cosmogenic nuclide research from the CRONUS Projects. Quat. Geochronol. 31, 155–159.
Reynolds, S.J., 1985. Geology of the South Mountains, central Arizona. Ariz. Bur. Geol. Miner. Technol. Bull. 195.
Seong, Y.B., Larson, P.H., Dorn, R.I., Yu, B.Y., 2016. Evaluating process domains in small granitic watersheds: case study of Pima Wash, South Mountains, Sonoran Desert, USA. Geomorphology 255, 108–124.
Sepulveda, S.A., Rebolledo, S., Vargas, G., 2006. Recent catastrophic debris flows in Chile: geological hazard, climatic relationships and human response. Quat. Int. 158, 83–95.
Sewell, R.J., Parry, S., Millis, S.W., Wang, N., Rieser, U., DeWitt, R., 2015. Dating of debris flow fan complexes from Lantau Island, Hong Kong, China: the potential relationship between landslide activity and climate change. Geomorphology 248, 205–227.
Shaw, R., 2015. Hazard, vulnerability and risk: the Pakistan context. In: Rahman, A.U., A.N., K., Shaw, R. (Eds.), Disaster Risk Reduction Approaches in Pakistan. Springer, Tokyo, pp. 31–52.
Spencer, J.E., 1984. The role of tectonic denudationin warping and uplift of low-angle normal faults. Geology 12, 95–98.
Stewart, B.A., Capo, R.C., Chadwick, O.A., 1998. Quantitative strontium isotope models for weathering, pedogenesis and biogeochemical cycling. Geoderma 82, 173–195.
Stolle, A., Langer, M., Blöthe, J.H., Korup, O., 2015. On predicting debris flows in arid mountain belts. Glob. Planet. Chang. 126, 1–13.
Tichavský, R., Šilhán, K., 2015. Dendrogeomorphic approaches for identifying the probable occurrence of debris flows and related torrential processes in steep headwater catchments: the Hrubý Jeseník Mountains, Czech Republic. Geomorphology 246, 445–457.
Webb, R.H., Leake, S.A., Malloy, R.A., 2013. Geologic, hydrologic, and urban hazards for design in desert environments. In: Malloy, R., Brock, J. (Eds.), Design with the Desert: Conservation and Sustainable Development. CRC Press, pp. 91–118.
Wells, S.G., McFadden, L.D., Dohrenwend, J.C., Bullard, T.F., Feilberg, B.F., Ford, R.L., Grimm, J.P., Miller, J.R., Orbock, S.M., Pickle, J.D., 1984. Late Quaternary geomorphic history of Silver Lake, eastern Mojave Desert, California: an example of the influence of climatic change on desert piedmonts. Surficial Geology of the Eastern Mojave Desert, California. Geological Society of America Field Guide 14 (Reno).
Yair, A., Klein, M., 1973. The influence of surface properties on flow and erosion processes on debris covered slopes in an arid area. Catena 1, 1–18.
Youberg, A., Cline, M.L., Cook, J.P., Pearthree, P.A., Webb, R.H., 2008. Geological mapping of debris-flow deposits in the Santa Catalina Mountains, Pima County, Arizona. Arizona Geological Survey Open File Report 08-06, pp. 1–47.
Yu, B., Zhu, Y., Wang, T., Zhu, Y., 2016. A 10-min rainfall prediction model for debris flows triggered by a runoff induced mechanism. Environ. Earth Sci. 75, 1–14.
Zerboni, A., 2008. Holocene rock varnish on the Messak plateau (Libyan Sahara): chronology of weathering processes. Geomorphology 102, 640–651.
Zhou, H., Wang, X., Wang, C., Yuan, Y., Wang, D., Xu, Y., Pan, J., Lair, K., Barnett, A., Kierath, S., 2016. Adapting against disasters in a changing climate. In: Nadin, R., Opitz-Stapleton, S., Xu, Y. (Eds.), Climate risk and resilience in China. Routledge, New York, pp. 63–94.